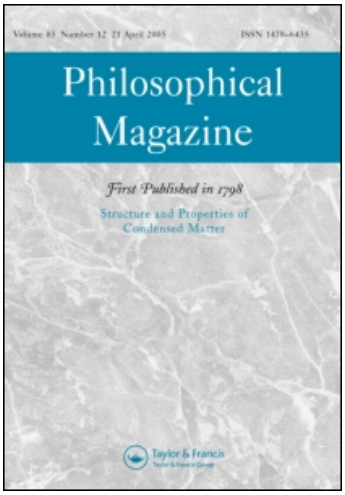

Philosophical Magazine
Publication details, including instructions for authors and subscription information:
http://www.informaworld.com/smpp/title~content=t713695589

Breakdown of semi-classical conduction theory in approximants of the octagonal tiling

G. Trambly de Laissardière[a]; C. Oguey[a]; D. Mayou[b]
[a] Laboratoire de Physique Théorique et Modélisation, CNRS UMR 8089, Université de Cergy-Pontoise, 95302 Cergy-Pontoise, France [b] Institut Néel, CNRS, Université Joseph Fourier, 38042 Grenoble Cedex 9, France

First published on: 11 November 2010

To cite this Article de Laissardière, G. Trambly , Oguey, C. and Mayou, D.(2010) 'Breakdown of semi-classical conduction theory in approximants of the octagonal tiling', Philosophical Magazine,, First published on: 11 November 2010 (iFirst)
To link to this Article: DOI: 10.1080/14786435.2010.523718
URL: http://dx.doi.org/10.1080/14786435.2010.523718

Philosophical Magazine
2010, 1–9, iFirst

Breakdown of semi-classical conduction theory in approximants of the octagonal tiling

G. Trambly de Laissardière[a]*, C. Oguey[a] and D. Mayou[b]

[a]*Laboratoire de Physique Théorique et Modélisation, CNRS UMR 8089, Université de Cergy-Pontoise, 2 av. A. Chauvin, 95302 Cergy-Pontoise, France;* [b]*Institut Néel, CNRS, Université Joseph Fourier, Bât D, 25 av. des Martyrs, B.P. 166, 38042 Grenoble Cedex 9, France*

(*Received 30 June 2010; final version received 9 September 2010*)

We present numerical calculations of quantum transport in perfect octagonal approximants. These calculations include a Boltzmann (intra-band) contribution and a non-Boltzmann (inter-band) contribution. When the unit cell size of the approximant increases, the magnitude of the Boltzmann terms decreases, whereas the magnitude of the non-Boltzmann terms increases. This shows that, in large approximants, the non-Boltzmann contributions should dominate the transport properties of electrons. This confirms the breakdown of the Bloch–Boltzmann theory for understanding the transport properties in approximants with very large unit cells, and then in quasicrystals, as found in actual Al-based approximants.

Keywords: quasicrystals; electronic transport; quantum critical phenomena; numerical simulation

1. Introduction

Since the discovery by Shechtman et al. [1], many experimental investigations have indicated that the conduction properties of several stable quasicrystals (AlCuFe, AlPdMn, AlPdRe, ...) are the opposite of those of good metals [2,3]. It appears also that the medium-range order, over one or a few nanometres, is the real length-scale that determines conductivity. In particular, the role of transition elements enhancing localisation has often been studied [4–11]. There is now strong evidence that these non-standard properties result from a new type of breakdown of the semi-classical Bloch–Boltzmann theory of conduction [12,13]. On the other hand, the specific role of long-range quasiperiodic order in transport properties is still an open question in spite of a large number of studies (see [8,14–23] and references therein). In this paper, we study 'how electrons propagate' in approximants of the octagonal tiling. This

*Corresponding author. Email: guy.trambly@u-cergy.fr

ISSN 1478–6435 print/ISSN 1478–6443 online

DOI: 10.1080/14786435.2010.523718
http://www.informaworld.com

tiling is one of the well-known quasiperiodic tilings that have been used to understand the influence of quasiperiodicity on electronic transport [14–17,19–21]. The main objective is to show that non-standard conduction properties result from purely quantum effects due to quasiperiodicity which cannot be interpreted through the semi-classical theory of transport.

2. The octagonal tiling and its approximants

The octagonal, or Ammann–Beenker, tiling [24,25] is a quasiperiodic tiling analogous to the well-known Penrose tiling. It has eight-fold C_{8v} point symmetry, inflation symmetry with ratio $\lambda = 1 + \sqrt{2}$, quasiperiodic translation symmetry, and Bragg peaks indexed by $\mathbb{Z}^4$. Those symmetries were observed in quasicrystalline phases of CrNiSi and AlMnSi alloys [26].

A sequence of periodic approximants $X_0, X_1, \ldots, X_k, \ldots$ can be generated by the inflation mapping M, operating as an invertible integer matrix on $\mathbb{Z}^4$ [27]. In the physical Euclidean plane E, and in the simplest version where the atoms occupy the tiling vertices, all the (atomic) sites have integer coordinates in the basis (e_1, e_2, e_3, e_4), where (e_1, e_2) forms an orthogonal basis of E and (e_3, e_4) is another orthogonal basis related to the former by a 45° rotation. All the tiles are congruent to either a square or a rhombus with 45° acute angle.

For $k = 0, 1, 2, \ldots$, the kth approximant is periodic, invariant under the translation lattice $\mathcal{L}_k$ generated by $\lambda^k e_1$ and $\lambda^k e_2$ (the square lattice $[e_1, e_2]$ dilated by a factor $L_k = \lambda^k$). In terms of the Pell, or 'octonacci', number sequence $P = \{P_k\} = \{0, 1, 2, 5, 12, \ldots\}$, defined by $P_0 = 0$, $P_1 = 1$, $P_{k+1} = 2P_k + P_{k-1}$, the unit cell contains $N_k = P_{2k+1} + P_{2k}$ vertices. Those vertices are given by the following construction: $\lambda^k(W_k \cap [e_3, e_4])$, i.e. select and expand sites of the square lattice $[e_3, e_4]$, and eventually bring them back into the square fundamental domain by $\mathcal{L}_k$ translations. The selection window W_k is a semi-regular octagon obtained as a projection of the 4D unit cube. Up to a sign $(-1)^k$, W_k is the span (all combinations with coordinates between 0 and 1) of the four vectors

$$P_k(e_4 - e_3), \quad -P_k(e_3 + e_4), \quad (P_k + P_{k-1})e_3, \quad (P_k + P_{k-1})e_4.$$

Duneau et al. [27] provide a slightly more efficient numerical method, avoiding useless scans, by partitioning the octagon into six parallelogram subdomains; then each selection reduces to specifying ranges for the integer coordinates of a suitable lattice, followed by a global affine transformation.

The first approximant X_0 is a simple square tiling. In all subsequent approximants $k \geq 1$, the configurations around vertices are the same as in the octagonal quasiperiodic tiling, displayed in Figure 1. Only the approximants X_1 contain incomplete subsets of these six local patterns, depending on the phase.

In units of edge length $a = ||e_j||$, the shortest distances between vertices are $1/\sqrt{2}, 1, \sqrt{2}$, corresponding to the short rhombus diagonal, the tile edge and the square diagonal, respectively.

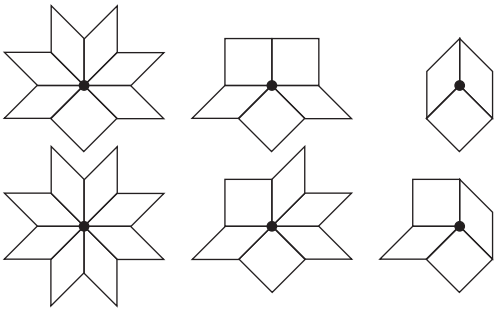

Figure 1. Vertex configurations of the octagonal tiling and of its approximants $k \geq 1$.

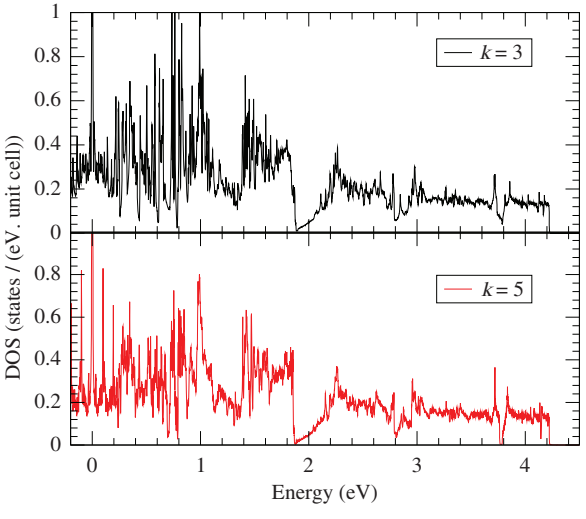

Figure 2. Total density of states in perfect octagonal approximants $k = 3$ and $k = 5$. The DOS is symmetric with respect to $E = 0$ [20].

3. Electronic structure

We study a pure hopping Hamiltonian

$$H = \gamma \sum_{\langle i,j \rangle} |i\rangle \langle j|, \tag{1}$$

where i indexes s orbitals located on all vertices and $\gamma = 1$ eV is the strength of the hopping between orbitals. $\langle i, j \rangle$ are the nearest-neighbours at tile edge distance a (Figure 1). The properties of this model depend only on the topology of the tiling. The total density of states (total DOS), $n(E)$, is computed by a recursion method [22] in a large super-cell containing more than about 10 million orbitals. The DOS is shown in Figure 2. As already shown by Zijlstra [20], the DOS is spiky at the centre of the band ($|E| < 2$) and smooth near the band edges ($|E| > 2$).

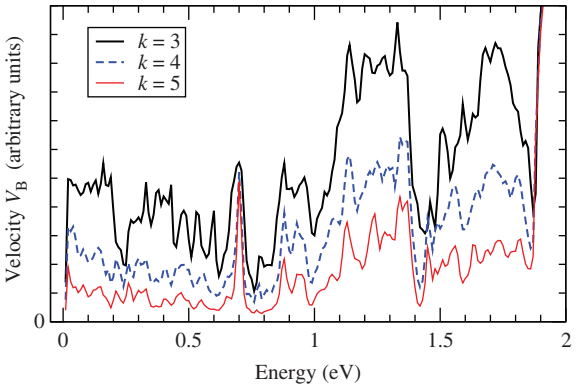

Figure 3. Average Boltzmann velocity V_B in perfect octagonal approximants $k=3$, $k=4$ and $k=5$.

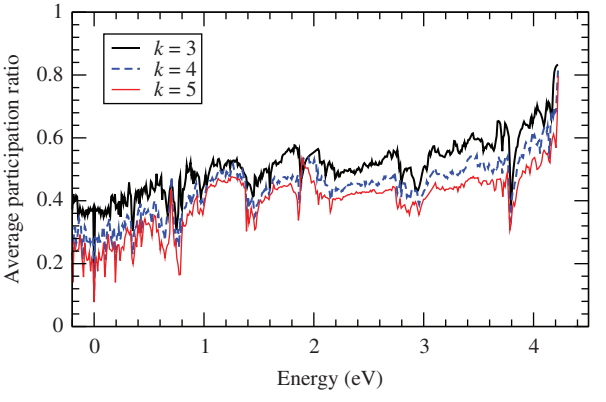

Figure 4. Average participation ratio $\tilde{p}(E)$ in perfect octagonal approximants $k=3$, $k=4$ and $k=5$.

The Boltzmann velocity (intra-band velocity) $V_B \propto \partial E_n(q)/\partial q$ (q is the wavevector) is shown in Figure 3. When the size of the approximant increases, V_B decreases as expected from band scaling analysis [14]. In order to quantify this localisation phenomenon, we compute the participation ratio of each eigenstate $|\psi\rangle$ defined by

$$p(\psi) = \left(N \sum_{i=1}^{N} |\langle i|\psi\rangle|^4 \right)^{-1}, \tag{2}$$

where i indexes orbitals in a $\mathcal{L}_k$ unit cell and $N(\equiv N_k)$ is the number of atoms in this unit cell. For completely delocalised eigenstates, p is equal to 1. On the other hand, states localised on one site have a small p value: $p = 1/N$. The average participation ratio $\tilde{p}(E)$ of all states with energy close to E is presented in Figure 4.

This figure shows clearly a stronger localisation of electronic states for larger approximants (larger k values).

4. Quantum diffusion

In the framework of the Kubo–Greenwood approach for calculation of the conductivity, the central quantities are the velocity correlation function of states of energy E at time t,

$$C(E,t) = \Big\langle V_x(t)V_x(0) + V_x(0)V_x(t)\Big\rangle_E = 2\,\mathrm{Re}\Big\langle V_x(t)V_x(0)\Big\rangle_E, \tag{3}$$

and the average square spreading of states of energy E at time t along the x-direction,

$$\Delta X^2(E,t) = \Big\langle \Big(X(t) - X(0)\Big)^2\Big\rangle_E. \tag{4}$$

In (3), Re A is the real part of A and $V_x(t)$ is the Heisenberg representation of the velocity operator V_x along x-direction at time t:

$$V_x = \frac{1}{i\hbar}\Big[X, H\Big]. \tag{5}$$

$C(E,t)$ is related to quantum diffusion by

$$\frac{\mathrm{d}}{\mathrm{d}t}\Big(\Delta X^2(E,t)\Big) = \int_0^t C(E,t')\mathrm{d}t'. \tag{6}$$

At zero temperature, the static conductivity is given by the Einstein formula,

$$\sigma = e^2 n(E_\mathrm{F}) D(E_\mathrm{F}), \tag{7}$$

where E_F is the Fermi energy and D is the diffusivity. In a perfect tiling at temperature $T = 0\,\mathrm{K}$,

$$D(E) = \frac{1}{2}\frac{d}{dt}\Delta X^2(E,t). \tag{8}$$

Once the band structure has been calculated from the tight-binding Hamiltonian (1) the velocity correlation function can be computed exactly in the basis of Bloch states [12,28]. Relation (6) shows that the anomalous behaviour of $C(E,t)$ also implies the anomalous behaviour of the quantum diffusion. In crystalline approximants, after a long time, when the spreading of states, $\Delta X = \sqrt{\Delta X^2}$, reaches the size L_k of a unit cell, the propagation should become ballistic. This means that the time averages at long times are $C(E,t) \simeq 2V_\mathrm{B}^2$ and $\Delta X^2(E,t) \simeq V_\mathrm{B}^2 t^2$, with V_B the Boltzmann velocity along the x-direction. But for smaller time values, when $\Delta X < L_k$, the spreading of states depends only on the tiling structure within a unit cell, which is closely related to quasiperiodicity. Therefore, an analysis of electron propagation in approximants on time range before the ballistic regime gives a good indication of how electrons propagate in a quasiperiodic structure.

As shown in Figure 5, the velocity correlation function in approximants can take negative values at some times, indicating the presence of back-scattering effects in

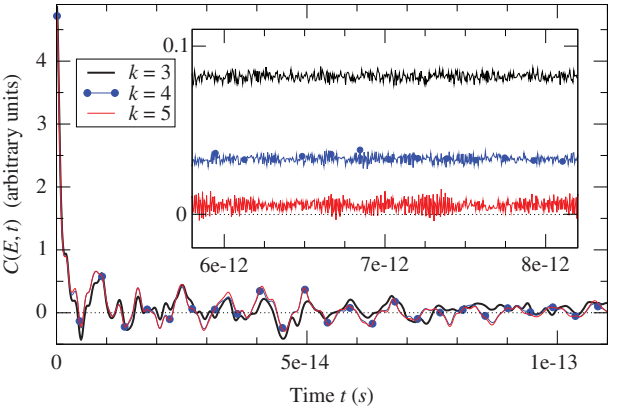

Figure 5. Velocity correlation function $C(E, t)$ versus time t in perfect octagonal approximants $k = 3$, $k = 4$ and $k = 5$. For $E = 0.5$ eV. Insert: same curves for large time values.

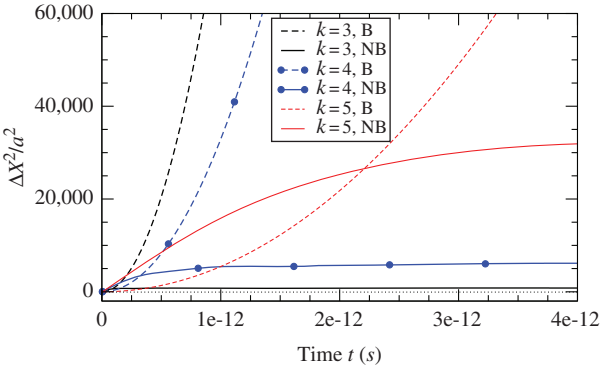

Figure 6. Boltzmann (ΔX^2_{B}) and non-Boltzmann (ΔX^2_{NB}) square spreading versus time t at $E = 0.5$ eV in perfect octagonal approximants $k = 3$, $k = 4$ and $k = 5$. a is the length of the edges of the tiling.

electron propagation. The decay of the Boltzmann term when k increases suggests that, for larger approximants, back-scattering ($C(E, t) < 0$) should be obtained even at some large time values. In that case, conductivity of the tiling will be strongly affected by this back-scattering phenomenon (Equation (8)).

The average square spreading is the sum of two terms (Figure 6):

$$\Delta X^2(E, t) = V_{\mathrm{B}}^2 t^2 + \Delta X^2_{\mathrm{NB}}(E, t). \tag{9}$$

The first term is the ballistic (intra-band) contribution at the energy E. The semi-classical model of Bloch–Boltzmann theory is equivalent to taking into account only this first term. The second term (inter-band contributions) $\Delta X^2_{\mathrm{NB}}(E, t)$ is a non-ballistic (non-Boltzmann) contribution. It is due to the non-diagonal elements of the velocity operator and describes the spreading of the wavefunction in a cell. This term is bounded by $L_m(E)^2$, which depends on the energy E [28]. From numerical

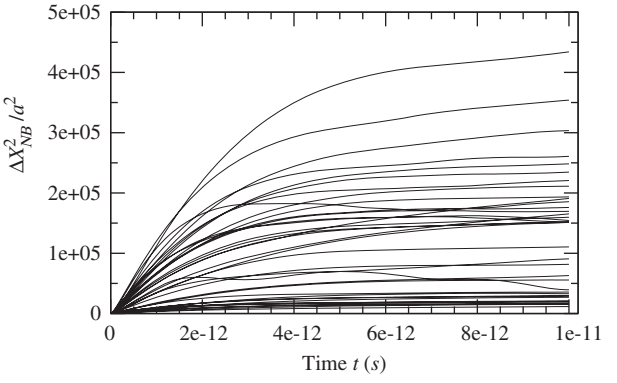

Figure 7. Non-Boltzmann square spreading ΔX^2_{NB} versus time t at different energies E in perfect octagonal approximant $k=5$. a is the tile edge length.

calculations, it is found that $\Delta X^2_{\mathrm{NB}}(E,t)$ rapidly reaches its maximum limit $\sim L_m(E)^2$ (Figure 7). Moreover, for many energies, numerical calculations show that $L_m(E)$ is of the order of magnitude of the unit cell size L_k or less (see also [12]). It suggests that in approximants the medium-range order partially localises electron states and this phenomenon should lead to anomalous diffusion in quasicrystalline phases. For large time ($t > L_m/V_{\mathrm{B}}$) the ballistic contribution dominates, but for small time ($t < L_m/V_{\mathrm{B}}$) the non-ballistic contribution could dominate (the 'small velocity regime' [12]). When the size of the approximants increases, the characteristic time L_m/V_{B} of the crossover between ballistic and non-ballistic behaviour increases.

In the relaxation time approximation [12,13,28,29], the role of phonons and static defects is taken into account by a scattering time τ. τ decreases when the temperature T increases and when the number of static defects increases. The velocity correlation function C' at temperature T and/or with static defects is computed from C at $T=0\,\mathrm{K}$ in a perfect tiling,

$$C'(E,t) = C(E,t)\mathrm{e}^{-|t|/\tau}. \tag{10}$$

Here the Fermi–Dirac distribution function is taken to be equal to its zero temperature value. This is valid provided that the electronic properties vary smoothly on the thermal energy scale $k_{\mathrm{B}}T$. The static diffusivity D' is then [28]

$$D'(E_{\mathrm{F}},\tau) = \frac{1}{2}\int_0^{+\infty} C(E_{\mathrm{F}},t)\mathrm{e}^{-t/\tau}\,\mathrm{d}t. \tag{11}$$

Roughly speaking, the transport properties are almost entirely determined by $\Delta X^2(E_{\mathrm{F}}, t=\tau)$. Therefore, in large approximants for which ($\tau < L_m/V_{\mathrm{B}}$), transport properties will be governed by non-ballistic (non-metallic) behaviour. Figure 8 shows the diffusivity in approximant $k=5$, calculated in the relaxation time approximation. D' is the sum of a ballistic term, $D'_{\mathrm{B}} \propto \tau$, and a non-ballistic term, D'_{NB}. For small τ value, its behaviour is not ballistic ($D' \neq D'_{\mathrm{B}}$). In larger approximants ($k > 5$), one can expect an 'insulating like' behaviour (D' decreases when τ increases) for a realistic range of τ values, like that found in real approximants [12].

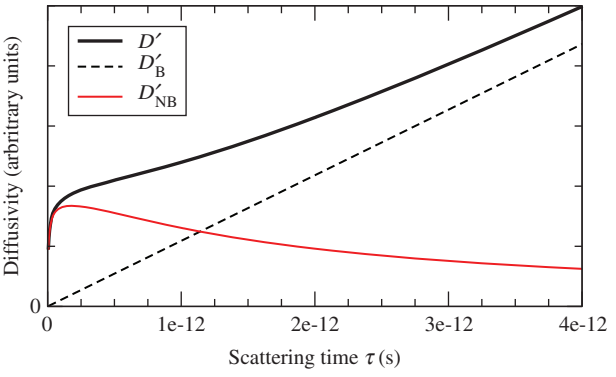

Figure 8. Diffusivity D', in the relaxation time approximation, versus scattering time τ, at $E_F = 0.5$ eV in octagonal approximant $k = 5$. $D' = D'_B + D'_{NB}$.

5. Conclusion

To summarise, we have presented quantum diffusion by a pure hopping Hamiltonian in approximants of an octagonal tiling ($k \leq 5$). When the size of the approximant increases the usual Boltzmann term decreases rapidly and new non-Boltzmann terms become essential to understand transport properties. These non-Boltzmann terms can have 'insulating like' behaviour, suggesting that in larger approximants ($k > 5$), 'insulating like' states, due to long-range quasiperiodic order, could exist. Calculations in larger approximants are in progress.

Acknowledgements

The computations have been performed at the Service Informatique Recherche (S.I.R.), Université de Cergy-Pontoise. We thank Y. Costes, S.I.R., for computing assistance.

References

[1] D. Shechtman, I. Blech, D. Gratias and J.W. Cahn, Phys. Rev. Lett. 53 (1984) p.1951.
[2] S.J. Poon, Adv. Phys. 41 (1992) p.303.
[3] C. Berger, *Electronic properties of quasicrystals, experimental*, in *Lectures on Quasicrystals*, F. Hippert and D. Gratias, eds., Editions de Physique, Les Ulis France, 1994, p.463.
[4] A. Pastuel, D.N. Manh and D. Mayou, J. Phys. Chem. Solids 47 (1986) p.325.
[5] T. Fujiwara, Phys. Rev. B 40 (1989) p.942.
[6] T. Fujiwara, S. Yamamoto and G. Trambly de Laissardière, Phys. Rev. Lett. 71 (1993) p.4166.
[7] M. Krajčí, J. Windisch, J. Hafner, G. Kresse and M. Mihalkovič, Phys. Rev. B 51 (1995) p.17355.
[8] T. Fujiwara, T. Mitsui and S. Yamamoto, Phys. Rev. B 53 (1996) p.R2910.
[9] G. Trambly de Laissardière and D. Mayou, Phys. Rev. B 55 (1997) p.2890.
[10] G. Trambly de Laissardière, S. Roche and D. Mayou, Mater. Sci. Eng. A 226 (1997) p.986.

[11] G. Trambly de Laissardière, D. Nguyen-Manh and D. Mayou, Prog. Mater Sci. 50 (2005) p.679.
[12] G. Trambly de Laissardière, J.P. Julien, and D. Mayou, Phys. Rev. Lett. 97 (2006) p.026601.
[13] G. Trambly de Laissardière, J.-P. Julien and D. Mayou, Phil. Mag. 88 (2008) p.2131.
[14] C. Sire and J. Bellissard, Europhys. Lett. 11 (1990) p.439.
[15] B. Passaro, C. Sire and V.G. Benza, Phys. Rev. B 46 (1992) p.13751.
[16] A. Jagannathan, J. Phys. I France 4 (1994) p.133.
[17] J.X. Zhong and R. Mosseri, J. Phys. I France 4 (1994) p.1513.
[18] S. Roche and D. Mayou, Phys. Rev. Lett. 79 (1997) p.2518.
[19] E.S. Zijlstra, Phys. Rev. B 66 (2002) p.214202.
[20] E.S. Zijlstra, J. Non-Cryst. Solids 334 (2004) p.126.
[21] A. Jagannathan and F. Piechon, Phil. Mag. 87 (2007) p.2389.
[22] F. Triozon, J. Vidal, R. Mosseri, and D. Mayou, Phys. Rev. B 65 (2002) p.220202.
[23] S. Yamamoto and T. Fujiwara, Phys. Rev. B 51 (1995) p.8841.
[24] R. Ammann, B. Grünbaum and G.C. Shephard, Discrete Comput. Geom. 8 (1992) p.1.
[25] J.E.S. Socolar, Phys. Rev. B 39 (1989) p.10519.
[26] Z.M. Wang and K.H. Kuo, Acta Cryst. A 44 (1988) p.857.
[27] M. Duneau, R. Mosseri and C. Oguey, J. Phys. A Math. Gen. 22 (1989) p.4549.
[28] D. Mayou and G. Trambly de Laissardière, *Quantum transport in quasicrystals and complex metallic alloys,* in *Quasicrystals*, T. Fujiwara and Y. Ishii, eds., Elsevier, Amsterdam, 2008, p.209.
[29] D. Mayou, Phys. Rev. Lett. 85 (2000) p.1290.